Published in final edited form as:
IEEE Trans Ultrason Ferroelectr Freq Control. 2012 October ; 59(10): 2312–2321. doi:10.1109/TUFFC.2012.2456.

Crosstalk Reduction for High-Frequency Linear-Array Ultrasound Transducers Using 1–3 Piezocomposites With Pseudo-Random Pillars

Hao-Chung Yang,
The National Institutes of Health Transducer Resource Center and Department of Biomedical Engineering, University of Southern California, Los Angeles, CA

Jonathan Cannata,
HistoSonics Inc., Ann Arbor, MI.

Jay Williams, and
The National Institutes of Health Transducer Resource Center and Department of Biomedical Engineering, University of Southern California, Los Angeles, CA

K. Kirk Shung
The National Institutes of Health Transducer Resource Center and Department of Biomedical Engineering, University of Southern California, Los Angeles, CA

Hao-Chung Yang: yangh@usc.edu

Abstract

The goal of this research was to develop a novel diced 1–3 piezocomposite geometry to reduce pulse–echo ring down and acoustic crosstalk between high-frequency ultrasonic array elements. Two PZT-5H-based 1–3 composites (10 and 15 MHz) of different pillar geometries [square (SQ), 45° triangle (TR), and pseudo-random (PR)] were fabricated and then made into single-element ultrasound transducers. The measured pulse–echo waveforms and their envelopes indicate that the PR composites had the shortest −20-dB pulse length and highest sensitivity among the composites evaluated. Using these composites, 15-MHz array subapertures with a 0.95λ pitch were fabricated to assess the acoustic crosstalk between array elements. The combined electrical and acoustical crosstalk between the nearest array elements of the PR array sub-apertures (−31.8 dB at 15 MHz) was 6.5 and 2.2 dB lower than those of the SQ and the TR array subapertures, respectively. These results demonstrate that the 1–3 piezocomposite with the pseudo-random pillars may be a better choice for fabricating enhanced high-frequency linear-array ultrasound transducers; especially when mechanical dicing is used.

I. Introduction

The 1–3 piezocomposites, which consist of an array of piezoelectric pillars embedded in a passive polymer matrix, are widely used in fabricating ultrasound imaging devices because of their enhanced electromechanical coupling efficients (k_t) and acoustic impedances when compared with solid piezoelectric ceramics and crystals [1]. Another advantage of 1–3 piezocomposites is that, unlike bulk piezoelectrics, their material properties, such as electrical and acoustic impedance, can be tailored to specific requirements. Finally, the need for an acoustic lens can be eliminated because piezocomposites are typically more flexible and can be easily geometrically shaped [2]–[4]. This is advantageous because commonly used lens materials such as urethane and epoxy can be very attenuative at high frequencies, and for array transducers, the lens can also cause significant degradation in beamforming [5].

Although the piezocomposites have several advantages over bulk piezoelectrics, their benefits come at the expense of introducing more undesired inter-pillar resonances. Auld and Smith [6] demonstrated that they may be due to the formation of Lamb waves in the periodic micro-structure of the piezocomposites. These resonances couple strongly with the fundamental thickness-mode resonance frequency and, hence, degrade the performance of the device; this is especially true for using the composites to fabricate linear-array transducers because they are more susceptible to crosstalk (mechanical and electrical coupling) between array elements. The resonances cause elements not to operate independently but together, leading to changes in the beam pattern, electrical impedance, and echo response [7]–[9].

The conventional solution to this problem is to make the kerf- and pillar-widths sufficiently small so as to ensure that the frequencies of these lateral resonances are at least double that of the transducer's fundamental frequency [10]. The most common method for the fabrication of 1–3 piezocomposites is the dice-and-fill technique, in which a plate of piezoelectric material is diced using a mechanical saw and a polymer is applied and then cured within the kerfs. However, as the frequency of operation increases, the desired kerf and pillar-widths decrease sharply; for instance, the required kerf for a 20-MHz 1–3 piezocom-posite is less than 10 μm, which is smaller than the width of the thinnest blade currently available for commercial dicing saws. Therefore, for the mechanical dice-and-fill technique, the fabrication of fine-scale composites which are immune to the deleterious effects of lateral resonances is still very challenging.

Recently, a modified dice-and-fill process, interdigital pair bonding (IPB) [11], was used to fabricate fine-scale composites with approximately 19-μm-wide pillars separated by 6-μm-wide kerfs [12]; however, this method is extremely time-consuming. In addition, because the piezo-composite properties are largely determined by the shear properties of filler epoxy [10], Brown *et al.* [5] used a very soft epoxy as the matrix of the piezo-composite to significantly minimize the lateral resonances. This soft epoxy provided good pillar-to-pillar damping across the composite; however, the soft epoxy was not able to resist high voltage during poling, causing potential short-circuits of the device. This drawback is especially critical for the high-frequency composite array transducers, which typically have numerous fine-scale kerfs. Many alternative methods also have been employed to obtain high volume fractions and small pillar- and kerf- widths, such as laser dicing [13] and reactive ion etching [14]. However, these methods are costly and lack the ability to produce pillars with uniform aspect ratios.

To develop alternate methods of lateral resonance suppression, Hossack, Hayward, and colleagues compared low-frequency piezocomposites of different pillar geometries from 1991 to 1996 [15]–[17]. They found that triangular pillars have the potential for improved electromechanical characteristics when they are oriented to avoid facing parallel surfaces. Furthermore, for a 1–3 composite with triangular pillars, when its surface dilation homogeneity (a measure of how uniformly the pillar-epoxy surface vibrates in the thickness mode) decreases below 90%, the efficiency of the composite decreases severely. Therefore, to keep the surface dilation homogeneity above 90%, Hay-ward proposed a set of criteria, maximum pillar aspect ratio (MPAR), to push the frequency of the first lateral resonance to at least 2 times the center frequency of the fundamental mode. Generally, an MPAR of approximately 0.4 was then required for a triangular pillar composite with a 40% ceramic volume fraction [17]. However, this criteria is not suitable for high-frequency mechanically diced 1–3 composites because it makes the fabrication of the 1–3 composites extremely difficult. In 2007, Brown *et al.* developed a 1–3 piezocomposite with mechanically diced triangular pillars (MPAR > 0.8) to reduce the influence of the lateral-mode resonances on the thickness-mode resonance within the composite by spreading the energy over a broad

frequency range [18]. Compared with the square pillar composites, the triangular pillar composites showed a 9.5 dB reduction in spurious signals and a 30% gain in the 2-way pulse bandwidth. In 2010, Yin *et al.* observed that lateral resonance suppression in piezocomposites with 45° triangular pillars was better than that of 30° and 60° triangular pillars which was attributed to a higher level of geometric complexity [19].

These observations imply that the highest level of geometric complexity translates to the greatest suppression of coupling between lateral- and thickness-mode resonances. Theoretically, the highest level of geometric complexity can be obtained using piezocomposites with distributed period pitches, such as randomly spaced/sized elements [20]–[22]. Hossack and Hayward tested this idea on several low-frequency 1–3 piezocomposites with a distributed period structure and demonstrated that no strongly coupled resonant frequencies were observed [15]. The aforementioned studies inspired us to develop and test a composite with a pseudo-random pillar geometry and distribution that could be used in the design of ultrasound transducers operating at frequencies up to 40 MHz. In addition, this composite geometry was developed so that a mechanical dicing saw could still be used for fabrication.

This paper first describes the design and fabrication of 1–3 piezocomposite with pseudo-random pillars. For comparison, we designed and fabricated several PZT-5H based 1–3 composites with different pillar geometries [square (SQ), 45° triangle (TR), and pseudo-random (PR); see Fig. 1]. A modified mechanical dicing technique has been used, whereby multiple dice-and-fill operations are performed to produce piezoelectric ceramic pillar spacing that would not have been possible with a single dicing operation [5], [23]. Using these composites, several ultrasound transducers were fabricated for comparison of acoustic performance. We then fabricated 15-MHz array subapertures with a 0.95λ pitch using these composites to compare acoustic crosstalk between array elements.

II. Composite Fabrication and Evaluation

The different pillar geometries (SQ, TR, and PR) fabricated for this study were designed to have a ceramic volume fraction of nearly 50% and kerf width, K, of 14 μm (see Table I). This design enabled us to compare the performance of these composites fairly, because the ceramic volume fraction of a composite determines the density and the permittivity [1], [6], [14]. To keep both the same ceramic volume fraction and the same kerf width for all three pillar geometries, the pillar widths, W, of the SQ, TR, and PR composites had to be kept at 34, 38, and 57 μm, respectively. The thickness, H, which corresponds to the antiresonant frequency of 10 MHz was 165 μm; for 15 MHz, it was 110 μm. Ideally, for low-volume-fraction composites, the pillar width-to-height ratios (W/H) must be less than approximately 0.5 to avoid the deleterious effects of mode-coupling [17]. The higher aspect ratio would lead to significant coupling between the lateral- and thickness-mode resonances. The maximum aspect ratios (the diagonal direction) of these composites, therefore, all remained below 0.5 except for the PR 15-MHz (0.52).

Commercial PZT-5H ceramic plates (3203Hd, CTS Electronic Components Inc., Albuquerque, NM) were diced into smaller square pieces (15 × 15 mm, 550 μm thick) which were then individually bonded onto flat glass carriers using low-temperature paraffin wax. A programmable dicing saw (Tcar 864–1, Thermocarbon Inc., Cassel-berry, Fl) was used to cut kerfs into these ceramic plates using a 12-μm blade. Because the vibration of the blade cannot be avoided, the resulting kerf widths in the composites will be slightly larger than the dicing saw blade thickness. Depending on the state of the blade, the resulting kerf width typically fluctuated between 12 and 14 μm.

Because the pillar scale was quite close to the machinability limit of the PZT-5H on our dicing saw, to decrease pillar breakage, a double-index-dicing technique was used to produce such fine-scale pillar spacing [23]. To keep the volume fraction constant for all different pillar geometries, different pillar widths and pitches were used; thus, we detail the fabrication processes for the different composite pillar geometries separately.

A. Square (SQ)

First, using the 12-μm dicing blade, two sets of cross cuts (200 μm deep) were first made into the ceramic at right angles to each other with a pitch of 96 μm. These first cuts were subsequently filled with Epotek 301 epoxy (Epoxy Technology Inc., Bellerica, MA) by capillary action. The filler in this first set was left to cure at room temperature in a dry nitrogen environment for three days. The excess epoxy was then lapped off to expose the diced ceramic. The second cuts were then made between these first cuts to produce the final 48-μm composite pitch. The second set of diced kerfs was subsequently filled in the same manner. After curing and lapping off the excess epoxy from the top of the composite, the composite was flipped over and then lapped down to 165 μm. The average width of the resultant kerfs was 14 μm, and the width of the ceramic pillars was 34 μm. The net piezoceramic volume fraction of this square pillar 1–3 composite was 50% [see Fig. 1(a)].

B. 45° Triangle (TR)

As with the square pillar composite, on the top of the ceramic, two sets of perpendicular cuts were first made in the ceramic 200 μm deep at a 73 μm pitch and then filled with epoxy. After curing, the second set of cuts was made at 45° angles relative to the vertical with a double modified pitch (2 × 51 μm) and then filled with epoxy again. After the epoxy had cured, the third set of cuts was then made between the second set of cuts to produce the final modified pitch (51 μm). This modified pitch kept the pitch (73 μm) between the first cuts constant over the entire surfiace of the composite. The resulting diced kerfs were subsequently filled with epoxy in the same manner. Because one more cut was required to fabricate the TR composites, it was more time-consuming than that of the SQ composites. The average resultant kerf width was 14 μm, and the width of the ceramic pillars was 46 μm, with a net piezoceramic volume fraction of 46% [see Fig. 1(b)]. For more detail about the fabrication of a 45° triangle 1–3 piezocomposite see yin *et al.* [19].

C. Pseudo-Random (PR)

The pseudo-random composite fabrication procedure was similar to the aforementioned processes for the square and the 45° triangle pillars. The differences were that two sets of cross cuts were first made at angles of 25° and 145° relative to the horizontal, with a pitch of 71 μm. This first set of cuts was then filled with Epotek 301 epoxy and cured at room temperature. The second set of cuts was subsequently made at an angle of 90° relative to the horizontal on the same surface with the same pitch. Because no third cut was required for the PR composites, it was the least time-consuming of the three composites fabricated. The maximum ceramic pillar width was 57 μm, and kerf width was 14 μm. The estimated piezoceramic volume fraction of this 1–3 composite was 49% [see Fig. 1(c)].

To determine how performance changes when the maximum aspect ratio for each composite increases, these composites were each cut in half. One half was used to fabricate the 10-MHz transducers, and the other half was then lapped down for the 15-MHz transducers. The top and bottom surfaces of all of the composites were then cleaned and sputtered (NSC-3000, Nano-Master Inc., Aus-tin, TX) with a total of 1000 Å of Cr/Au as a conduction layer. Each sample was poled in air at room temperature for 10 min using a dc field of Approximately 3 kV/mm. The electrical impedance of freestanding composites were measured with an impedance analyzer (4294a with 16034H test fixture, Agilent

Technologies, Santa Clara, CA); the results are shown in Fig. 2. The thickness mode electromechanical coupling coefficient (k_t), clamped dielectric loss tangent $\tan(\delta_e^S)$, mechanical quality factor (Q_m), attenuation coefficient (α), relative clamped permittivity ($\varepsilon_{33}^S/\varepsilon_o$), and longitudinal velocity (V_1) were calculated using measurements of air-resonating samples [24], [25] and a submicrometer thickness gauge (CT25/ND281b, Heidenhain Corp., Schaumburg, IL).

The measured electrical impedances, in Fig. 2, of the 10-MHz and 15-MHz 1–3 composites were compared. For the SQ and TR 10-MHz composites, a minor lateral resonance was visible at 20 MHz; however, no obvious lateral resonance was found on the PR 10-MHz composites. This might be attributed to the non-periodic structures within the PR composites. When the frequency was increased to 15 MHz, the fundamental frequency of the SQ composites combined with the first lateral resonance peak and the rest of lateral resonance peaks were found from 20 to 30 MHz though for the TR and PR 15-MHz composites, fewer lateral resonance peaks were found in the same frequency range. A comparison of the amplitude of the fundamental frequency peak with that of the highest lateral resonance peak shows that, at 15 MHz, the PR composites were less affected by the lateral resonance than the SQ and TR composites.

The piezoelectric properties of these composites were calculated from the measured electrical impedance (see Table II). The average of these properties was obtained from three samples of each of the composite pillar geometries. The results demonstrate that the PR composites had slightly higher relative clamped permittivity (493 at 10 MHz and 520 at 15 MHz). This is advantageous for the composite transducer with a small aperture size because higher relative clamped permittivity may better match the 50-Ω electrical impedance of commercial systems. Furthermore, the PR composites have higher k_t values (0.62 at 10 MHz and 0.61 at 15 MHz) than the SQ and TR composites. Study provides evidence that, for a free-standing PZT bar, k_t increases to its maximum at around an aspect ratio of 0.6 [26]. The fact that PR composites have greater maximum aspect ratios (0.35 at 10 MHz and 0.52 at 15 MHz) may lead to the higher k_t values. Moreover, this enhanced k_t value may be attributed to the greater distribution of pillar resonance frequencies resulting from the varying pillar widths.

Additionally, although the maximum aspect ratio for the PR composites was higher than those of the SQ and TR composites, the PR composites still out performed them. This observation implies that the PR composites may have a higher limit for the maximum aspect ratio. This would be advantageous for fabricating high-frequency transducers. Therefore, the PR composites may not only suppress the lateral interference better than the SQ composites, but also provide a higher k_t than the TR composites. To further investigate the frequency response properties of the single-element transducers fabricated from these composites, we then measured their pulse–echo results.

III. Composite Transducer Fabrication and Evaluation

A. Single-Element Composite Transducers: Pulse–Echo Measurement

Single-element transducers were fabricated first by bonding conductive epoxy (E-Solder 3022, Von Roll Isola Inc., New Haven, CT) backing material to the composite. The resulting plates were mechanically shaped into 2.5mm disks using a lathe and then made into single-element ultrasound transducers. A prefabricated Epotek 301 epoxy sheet (Z = 3.04 Mrayl, 66 μm for 10 MHz and 44 μm for 15 MHz) matching layer was bonded to the front face of the composite transducers. A cross-sectional diagram of the single-element ultrasound transducer is shown in Fig. 3. More details about the design and fabrication of this ultrasound transducer were reported elsewhere [27].

The center frequency, bandwidth, pulse length, and two-way sensitivity of each composite transducer were measured by a common two-way pulse–echo test. A Panametrics 5900 pulser/receiver (Olympus NDT Inc., Waltham, MA) was used to excite each transducer at the 1 μJ, 50-Ω settings with no gain. The transducer was positioned in a degassed/deionized water bath opposite a flat quartz reflector. The echoes from the transducer were then digitized and displayed with a 500-MHz oscilloscope (LC534, LeCroy Corp., Chestnut Ridge, NY). Fast Fourier transform (FFT) of the echo yielded the frequency response of the echo. The upper and lower frequencies of the signal corresponded to the first and the second −6-dB points of this power spectrum, respectively. The mean of these frequencies was recorded as the center frequency of the transducers, and dividing the difference of the frequencies by the center frequency gives the bandwidth of the transducers. The amplitude of the echo signal was recorded for relative element sensitivity comparisons. The length of time between the first and last points where the signal was −20 dB relative to the peak was recorded as the −20-dB pulse length of the echo waveform.

The measured pulse-echo waveforms, their spectra and envelopes (see Fig. 4) of these composite transducers showed that, for instance, the SQ 10-MHz device had the longest −20-dB pulse length (282 ns), and the TR 10-MHz device had a shorter −20-dB pulse length (239 ns) but lower sensitivity (0.48 V). Note that the PR 10-MHz device had the shortest −20-dB pulse length (230 ns) and the strongest sensitivity (0.60 V). At 15 MHz, the −20-dB pulse length of the TR 15-MHz device was 140 ns, which was about 30 and 10 ns less than those of the SQ 15-MHz and the PR 15-MHz, respectively, but the PR 15-MHz still had the strongest sensitivity (0.75 V). This observation indicates that the TR and PR composites both were able to reduce the −20-dB pulse length better than the SQ composites and that the PR composites were the most sensitive. In addition, with or without a matching layer, the TR and PR composites have wider −6-dB bandwidth than the SQ composites. Table III summarizes the measured frequency response properties for these composites transducers with different pillar geometries.

B. Composite Array Transducer Subapertures

Next, we fabricated 15-MHz subaperture arrays consisting of 16 elements and approximately 0.95λ pitch (144 μm) from these composites to measure the acoustic crosstalk between elements. The orientation of elements relative to composite for each type is shown in Fig. 5. We separated the array elements by mechanically dicing off the top electrode layer over the composite kerfs to the depth of 1 μm with a 10-μm-wide dicing blade. Subsequently, we used an intermediate flexible circuit incorporating 5-μm-thick copper traces on a 25-μm-thick polyimide surface to connect individual coaxial cables to each array element. The flexible circuit was connected to each composite by carefully aligning and bonding the copper traces to the top electrodes with Epotek 301 epoxy. This interconnected array assembly was allowed to cure for 48 h at room temperature in A dry nitrogen environ- ment before further processing. After curing, an additional 1000-Å Cr/Au electrode was sputtered to connect the ground side of the composites to the flexible circuit. A 44-μm-thick prefabricated Epotek 301 epoxy sheet was bonded to the top surface of the composites as a matching layer. Another prefabricated backing block made of the same epoxy (7 mm thickness) was then bonded to the other side of the flexible circuit. The 7-mm backing thickness used was deemed acceptable to avoid backing echo interference based upon previously reported acoustic attenuation data [25]. Therefore, from top to bottom, the four layers of these subaperture arrays are the epoxy matching layer, the composite piezo-layer, the flexible circuit, and the epoxy backing layer. Then, 1-m-long, 75-Ω coaxial cables (measured impedance is $74.0 - 1.8i\,\Omega$, and capacitance per unit length is 64 pF/m) were soldered to the flexible circuit with a low-temperature, indium-based solder (Indium Corporation of America, Utica, NY). The completed array is shown in Fig. 6.

Identical coaxial cables connected the array elements to the electronics to provide equal loading conditions. These array subapertures were then placed in a deionized water bath with a flat quartz reflector. Because no dead element was found in these array subapertures, eight elements (Elements 1 to 8) of each the array subapertures were selected to represent all the elements.

1) Pulse–Echo Measurement—An identical two-way pulse–echo test was performed to measure pulse length of each array transducer subaperture. The Panametrics 5900 pulser/receiver (1 μJ, 50 Ω settings with no gain) was used to excite each transducer. The same flat quartz plate in a degassed/deionized water bath was used as a reflector. The echoes recorded by the transducer were then digitized and displayed with the LC534 oscilloscope. The frequency response of the echo was converted from the measured echo signal using fast Fourier transform (FFT). The pulse length of the echo waveform was recorded as the length of time between the first and last points where the signal was −20 dB relative to the peak. Table IV shows the measured −20-dB pulse length for the 15-MHz array subapertures. The PR array subaperture had the shortest −20-dB pulse length of 143.8 ns (SQ: 202.7 ns; TR: 151.2 ns).

2) Insertion Loss Measurement—Insertion loss is the ratio of the output power of the transducer to the input power delivered to the transducer from the source electronics. The two-way insertion loss for each element was recorded at 15 MHz. The amplitude of the sinusoidal signal (5 V_{pp} amplitude, 20 cycles) from an arbitrary function generator (AFG 3251, Tektronix Inc., richardson, TX), set in the burst mode, was measured (without the transducer) across a 50 Ω oscilloscope load at discrete frequencies from 3 to 30 MHz. These measured voltages served as the reference voltage. Each array element was then excited by the same function generator; and the echo signal peak amplitude was recorded at a distance of 11.5 mm (natural focus for the center element) on the oscilloscope across a 1 MΩ load. Measured two-way insertion loss was calculated using the ratio of the frequency spectrum of the transmitted and received responses, which compensated for the attenuation in the water bath (2.2×10^{-4} dB/mm·MHz^2) and loss caused by the imperfect reflection from the quartz target (1.8 dB). More details about the two-way insertion loss measurement were also presented elsewhere [28]. The average compensated insertion loss for the PR array subaperture (−24.2 dB) was lower than that of the SQ and TR array subapertures (−25.6 and −27.6 dB, respectively); see Table IV.

3) Crosstalk Measurement—The same function generator (AFG 3251, Tektronix) was set to sinusoid burst mode (5 V_{pp} amplitude) to excite each element of the array. Each element was excited at a step frequency of 1 MHz throughout the passband (3 to 30 MHz), and the peak applied voltage was recorded as a reference using the aforementioned oscilloscope set at 1 MΩ coupling. The echo signal peak amplitudes for all eight elements were mea- sured at a distance of 11.5 mm. Next, after the quartz reflector was removed, the voltages on the nearest-neighbor and next-nearest elements of each the element were also measured with the same oscilloscope (also set at 1 MΩ coupling) and compared with the reference voltage to determine the level of crosstalk [12]. For each element, its combined electrical and acoustical crosstalk was measured between its adjacent element and the next-nearest element. Fig. 7 shows average measured crosstalk (electrical and acoustical) between the nearest and next-nearest elements of these 15-MHz array subapertures. The crosstalk was averaged from the measurements of eight elements (Elements 1 to 8) of composite pillar geometry. Table V also summaries average crosstalk at 15 MHz and its standard deviation of each the composite pillar geometries. For the nearest elements, at 15 MHz the SQ array subaperture, as expected, had the highest level of crosstalk (−25.3 dB). Compared with the SQ array subaperture, the TR array subaperture reduced its combined crosstalk by 4.3 dB to

−29.6 dB. This observation also validated Brown and Yin's results [18], [19]. Notably, the PR array subaperture had the lowest measured crosstalk of −31.8 dB, which was 6.5 and 2.2 dB lower than that of the SQ and the TR array subapertures at the same frequency, respectively.

Between the next-nearest elements of these array subapertures, a similar reduced-crosstalk effect was also found. At 15 MHz, for instance, the PR array subaper- ture showed a combined crosstalk of −43.9 dB, which was 5.5 and 2.6 dB lower than that of the SQ and the TR array subapertures, respectively. Therefore, as expected, the PR pillar geometry significantly reduced the crosstalk between array elements.

IV. Discussion and Conclusions

This study is the first to report the fabrication and use of 1–3 composites with pseudo-random pillars to fabricate ultrasound transducers for the purpose of suppressing the lateral resonances and reducing the crosstalk between array elements. We compared different pillar geometries and found that the PR composites outperformed the others in specific categories. For example, the measured electrical impedance of these composites showed that the PR composites were less affected by the lateral resonance than the SQ and TR composites. In addition, compared with the SQ and TR composites, the PR composites had the highest relative clamped permittivity (520 at 15 MHz) and k_t values (~0.62).

For the PR composites, the level of geometric complexity is determined by the applied dicing angle sets (25° and 145° were adopted in this paper). There may be a Cor- relation between different dicing angle sets and the level of crosstalk between array elements; such as 45° and 135° or 35° and 145°. This could be evaluated in the future to determine ways to optimize the reduction of crosstalk between array elements.

Using these composites, several ultrasound transducers were fabricated to validate their acoustic performance in water. The measured pulse–echo waveforms and their envelopes showed that the TR and PR composite transducers both displayed shorter −20 dB pulse lengths when compared the SQ composite transducer, and the PR composite transducers were the most sensitive.

Additionally, 15-MHz array subapertures with a 0.95λ pitch were then developed using these composites to measure their acoustic crosstalk between array elements. Between the nearest elements, at 15 MHz the PR array subaperture had the lowest measured crosstalk, −31.8 dB, which was 6.5 and 2.2 dB lower than those of the SQ and the TR array subapertures, respectively. Overall, the PR composites outperformed the sq and TR composites in reducing the crosstalk between the array elements. We attribute the lowest crosstalk observed on the PR array subaperture mainly to its randomized composite pillars, which have the highest level of geometric complexity of the three composites. We hypothesize that the highest level of geometric complexity spreads the acoustic energy in all lateral directions within the composite; hence, as expected, the PR composite pillars minimizes the crosstalk between the array elements. Additionally, the PR composites are advantageous for fabricating high-frequency linear-array transducers because they had a higher maximum aspect ratio but still performed well. In the future, a study investigating the relationship between varying the dicing angle set and the crosstalk reduction may be desirable to optimize the reduction of the crosstalk between the array elements.

Finally, because of their larger pitch and semi-randomized geometry, the PR composites decreased the fabrication time but still performed well; therefore, when fabricating the high-frequency 1–3 composites, the PR pillar geometry has advantages over the SQ and TR in yield, convenience, and performance. Considering the observed piezoelectric properties and

acoustic performance, the results presented in this study suggest that 1–3 composites with pseudo-random pillars may be a better choice for the fabrication of high-frequency piezocomposite singleelement and array transducers. However, this work is an initial evaluation of this new composite geometry and more work, such as modeling with PZFlex (Weidlinger Associates Inc., Mountain View, CA), is needed for further analysis of its usefulness.

Acknowledgments

We thank Dr. C. Liu for his effort in fabricating the flexible circuits.

This work is based on research supported by National Institutes of Health grant number P41-EB2182.

References

1. Smith WA. New opportunities in ultrasonic transducers emerging from innovations in piezoelectric materials. Proc. SPIE Int. Symp. 1992; vol.1733:3–26.
2. Michau S, Mauchamp P, Dufait R. Piezocomposite 30 MHz linear array for medical imaging: Design challenges and performances evaluation of a 128 elements array. Proc. IEEE Ultrasonics Symp. 2004:898–901.
3. Zhao JZ, Alves CHF, Snook KA, Cannata JM, Chen WH, Meyer RJ Jr. Ayyappan S, Ritter TA, Shung KK. Performance of 50 MHz transducers incorporating fiber composite PVDF $PbTio_3$ and $LiNbO_3$. Proc. IEEE Ultrasonics Symp. 1999:1185–1189.
4. Lous GM, Cornejo IA, Mcnulty TF, Safari A, Danforth SC. Fabrication of curved ceramic/polymer composite transducer for ultrasonic imaging applications by fused deposition of ceramics. Proc. IEEE Ultrasonics Symp. 1998:239–242.
5. Brown JA, Foster FS, Needles A, Cherin E, Lockwood GR. Fabrication and performance of a linear array based on a 1–3 composite with geometric elevation focusing. IEEE Trans. Ultra-son. Ferroelectr. Freq. Control. 2007; vol. 54(no. 9):1888–1894.
6. smith WA, Auld BA. Modeling 1–3 composite piezoelectrics: Thickness-mode oscillations. IEEE Trans. Ultrason. Ferro-electr. Freq. Control. 1991; vol. 38(no. 1):40–47.
7. Certon D, Felix N, Lacaze E, Teston F, Patat F. Investigation of cross-coupling in 1–3 piezocomposite arrays. IEEE Trans. Ultrason. Ferroelectr. Freq. Control. 2001; vol. 48(no. 1):85–92. [PubMed: 11367810]
8. Baer RL, Kino GS. Theory for cross coupling in ultrasonic transducer arrays. Appl. Phys. Lett. 1984; vol. 44(no. 10):954–956.
9. Démoré CE, Brown JA, Lockwood GR. Investigation of cross talk in kerfless annular arrays for high-frequency imaging. IEEE Trans. Ultrason. Ferroelectr. Freq. Control. 2006; vol. 53(no. 5): 1046–1056. [PubMed: 16764458]
10. Reynolds P, Hyslop J, Hayward G. Analysis of spurious resonances in single and multi-element piezocomposite ultrasonic transducers. Proc. IEEE Ultrasonics Symp. 2003:1650–1653.
11. Liu R, Harasiewicz KA, Foster FS. Interdigital pair bonding for high frequency (20–50 MHz) ultrasonic composite transducers. IEEE Trans. Ultrason. Ferroelectr. Freq. Control. 2001; vol. 48(no. 1):299–306. [PubMed: 11367799]
12. Cannata JM, Williams JA, Zhang l, Hu CH, Shung KK. A high frequency linear ultrasonic array utilizing an inter-digitally bonded 2–2 piezo-composite. IEEE Trans. Ultrason. Fer-roelectr. Freq. Control. 2011; vol. 58(no. 10):2202–2212.
13. Lukacs M, Yin J, Pang G, Garcia RC, Cherin E, Williams R, Mehi J, Foster FS. Performance and characterization of new micromachined high-frequency linear arrays. IEEE Trans. Ultra-son. Ferroelectr. Freq. Control. 2006; vol. 53(no. 10):1719–1729.
14. Yuan JR, Jiang X, Cao PJ, Sadaka A, Bautista R, Snook K, Rehrig PW. High frequency piezo composites microfabri-cated ultrasound transducers for intravascular imaging. Proc. IEEE Ultrasonics Symp. 2006:264–268.

15. Hossack JA, Hayward G. Finite-element analysis of 1–3 composite transducers. IEEE Trans. Ultrason. Ferroelectr. Freq. Control. 1991; vol. 38(no. 6):618–629. [PubMed: 18267626]
16. Hamilton E, Hayward G. The Design of Low volume fraction composite transducers using finite element modeling techniques. Proc. IEEE Ultrasonics Symp. 1992:531–534.
17. Hayward G, Bennet J. Assessing the in fluence of pillar Aspect Ratio on the behavior of 1–3 Connectivity Composite transducers. IEEE Trans. Ultrason. Ferroelectr. Freq. Control. 1996; vol. 43(no. 1):98–108.
18. Brown JA, Cherin E, Yin J, Foster FS. Fabrication and performance of high-frequency composite transducers with triangular-pillar geometry. IEEE Trans. Ultrason. Ferroelectr. Freq. Control. 2009; vol. 56(no. 4):827–836. [PubMed: 19406712]
19. Yin J, Lee M, Brown JA, Cherin E, Foster FS. Effect of triangular pillar geometry on high-frequency piezocomposite transducers. IEEE Trans. Ultrason. Ferroelectr. Freq. Control. 2010; vol. 57(no. 4):957–968. [PubMed: 20378458]
20. Hossack JA, Auld BA, Batha HD. Techniques for suppressing spurious resonant modes in 1:3 composite transducers. Proc. IEEE Ultrasonics Symp. 1999:651–655.
21. Harvey G, Gachagan A, Mackersie J, Banks R. Exploring the advantages of a random 1–3 connectivity piezocomposite structure incorporating piezoelectric fibres as the active element. Proc. IEEE Ultrasonics Symp. 2006:1903–1906.
22. Yuan J, Marsh P, Liang K, Kunkel H. The dynamic characteristics of composites with periodic and random structure. Proc. IEEE Ultrasonics Symp. 1996:949–954.
23. cannata JM, Williams JA, Zhou Q, Ritter TA, Shung KK. Development of A 35-MHz piezo-composite ultrasound Array for medical imaging. IEEE Trans. Ultrason. Ferroelectr. Freq. Control. 2006; vol. 53(no. 1):224–236. [PubMed: 16471449]
24. Foster FS, Ryan LK, Turnbull DH. Characterization of lead zirconate titanate ceramics for use in miniature high-frequency (20–80 MHz) transducers. IEEE Trans. Ultrason. Ferroelectr. Freq. Control. 1991; vol. 38(no. 5):446–453. [PubMed: 18267606]
25. Wang H, Ritter TA, Cao W, Shung KK. High frequency properties of passive materials for ultrasonic transducers. IEEE Trans. Ultrason. Ferroelectr. Freq. Control. 2001; vol. 48(no. 1):78–84. [PubMed: 11367809]
26. Yin J, Lukacs M, Harasiewicz KA, Foster FS. Design and fabrication of ultrafine piezoelectric composites. Ultrason. Imaging. 2005; vol. 27(no. 1):54–64. [PubMed: 16003926]
27. Cannata JM, Ritter TA, Chen WH, Silverman RH, Shung KK. Design of efficient, broadband single-element (20–80 MHz) ultrasonic transducers for medical imaging applications. IEEE Trans. Ultrason. Ferroelectr. Freq. Control. 2003; vol. 50(no. 11):1548–1557. [PubMed: 14682638]
28. Ritter TA, Shrout TR, Tutwiler R, Shung KK. A 30MHz composite ultrasound array for medical imaging applications. IEEE Trans. Ultrason. Ferroelectr. Freq. Control. 2002; vol. 49(no. 2):217–230. [PubMed: 11885679]

Biographies

Hao-Chung Yang received his B.S. degree in mechanical engineering from the National Central University in Taiwan in 2001, his M.S. degree in engineering and system science from the National Tsing Hua University in Taiwan in 2003, and his Ph.D. degree in materials science from the University of Southern California, Los Angeles, CA, in 2012.

Since 2007, he has been working as a research assistant at the National Institutes of Health (NIH) Resource Center for Medical Ultrasonic Transducer Technology, University of

Southern California, Los Angeles, CA. His current research interests include the development of piezoelectric materials, and the design, modeling, and fabrication of ultrasonic transducers for medical applications.

Jonathan M. Cannata (S'01–M'04) received his B.S. degree in bioengineering from the University of California at San Diego in 1998, and his M.S. and Ph.D degrees in bioengineering from The Pennsylvania State University, University Park, PA, in 2000 and 2004, respectively.

From 2001 to 2011, Dr. Cannata served as the manager for the NIH Resource on Medical Ultrasonic Transducer Technology, which is currently located at the University of Southern California (USC). From 2005 to 2011, he held the title of Research Assistant Professor of Biomedical Engineering at USC.

Dr. Cannata's current position is Senior Ultrasound Engineer at Histosonics, Inc. There, he is working on a device for noninvasive surgery using ultrasound cavitation.

Jay A. Williams serves as a Transducer Engineer at the NIH Resource on Medical Ultrasonic Transducer Technology. Mr. Williams joined the group in March 2002 just prior to their move to the University of Southern California in August of that year. He has also been the webmaster for the Resource Center, http://bme.usc.edu/UTRC, since the move to USC. Some of his accomplishments include: the development of 128-element 25- to 30-MHz composite 30-μm-pitch phased arrays, 256-element 30-MHz composite 50-μm-pitch linear arrays, 64-element 35-MHz composite 50-μm-pitch linear arrays, 8-element 35- to 60-MHz annular arrays, very light-weight (<0.3 g 40- to 60-MHz, <0.2 g 80- to 100-MHz) high-frame-rate B-scan transducers, 100- to 150-MHz sputtered Zno transducers, and 10-MHz composite HIFU catheter transducers. He currently holds a patent, no. 7 695 784, covering post positioning for interdigital bonded composites. Mr. Williams audited courses in business management, computer science, mechanical engineering, architecture, and physics at The Pennsylvania state University from 1975 to 1977. He also achieved honors in both analog electronics at Radio Semiconductor, 1984, and digital electronics at Control Data Institute Multi-Skills Center, 1987. He had worked in industry for 25 years in a variety of technical fields, such as mass spec-trometry, microwave telecommunication, liquid chromatography, digital electronics, ultrasound, and information technology. In 1990, he began working in ultrasound at Blatek, Inc., State College, PA, serving 8 1/2 years in engineering, and then 2 1/2 years in management, including the last 5 years as IS/IT Manager, and the last 2 years as Quality System Manager, establishing their first ISO9001 and FDA CGMP (21CFr820) quality system. He has now worked in the ultrasound field for more than 20 years.

K. Kirk Shung obtained a B.S. degree in electrical engineering from Cheng-Kung University in Taiwan in 1968; an M.S. degree in electrical engineering from the University of Missouri, Columbia, MO, in 1970; and A Ph.D. in electrical engineering from the University of Washington, Seattle, WA, in 1975. He had taught at The Pennsylvania State University, University Park, PA, for 23 years before moving to the Department of Biomedical Engineering, University of Southern California, Los Angeles, CA, as a professor in 2002. He has been the director of the NIH Resource on Medical Ultrasonic Transducer Technology since 1997.

Dr. Shung is a life fellow of IEEE and a fellow of the Acoustical society of America and the American Institute of Ultrasound in Medicine. He is a founding fellow of the American Institute of Medical and Biological Engineering. He received the IEEE Engineering in Medicine and Biology society Early Career award in 1985, and was the coauthor of a paper that received the best paper award for the *IEEE Transactions on Ultrasonics, Ferroelectrics, and Frequency Control* (UFFC) in 2000. He was elected an outstanding alumnus of Cheng-Kung University in Taiwan in 2001. He was selected as the distinguished lecturer for the IEEE UFFC society for 2002–2003. He received the Holmes Pioneer award in basic science from the American Institute of Ultrasound in Medicine in 2010. He was selected to receive the academic career achievement award from the IEEE Engineering in Medicine and Biology society in 2011.

Dr. Shung has published more than 400 papers and book chapters. He is the author of the textbooks *Principles of Medical Imaging*, published by Academic Press in 1992, and *Diagnostic Ultrasound: Imaging and Blood Flow Measurements*, published by CRC Press in 2005. He coedited the book *Ultrasonic Scattering by Biological Tissues*, published by CRC Press in 1993. He is an associate editor of the *IEEE Transactions on Ultrasonics, Ferroelectrics, and Frequency Control* and a member of the editorial board of *Ultrasound in Medicine and Biology*. Dr. Shung's research interest is in ultrasonic transducers, high-frequency ultrasonic imaging, ultrasound microbeams, and ultrasonic scattering in tissues.

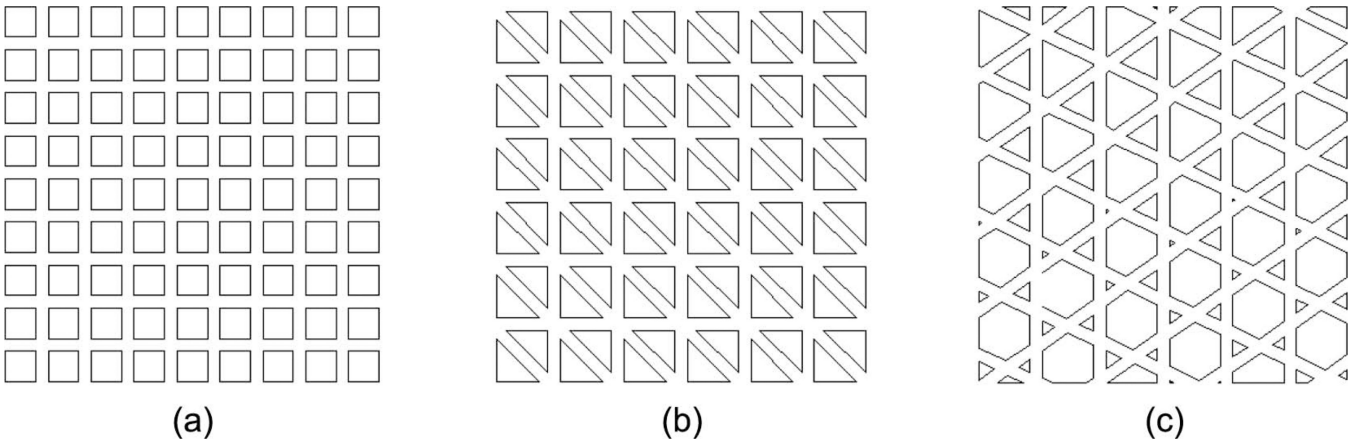

Fig. 1.
Different pillar geometries for the PZT-5H 1–3 composites: (a) square, (b) 45° triangle, and (c) pseudo-random.

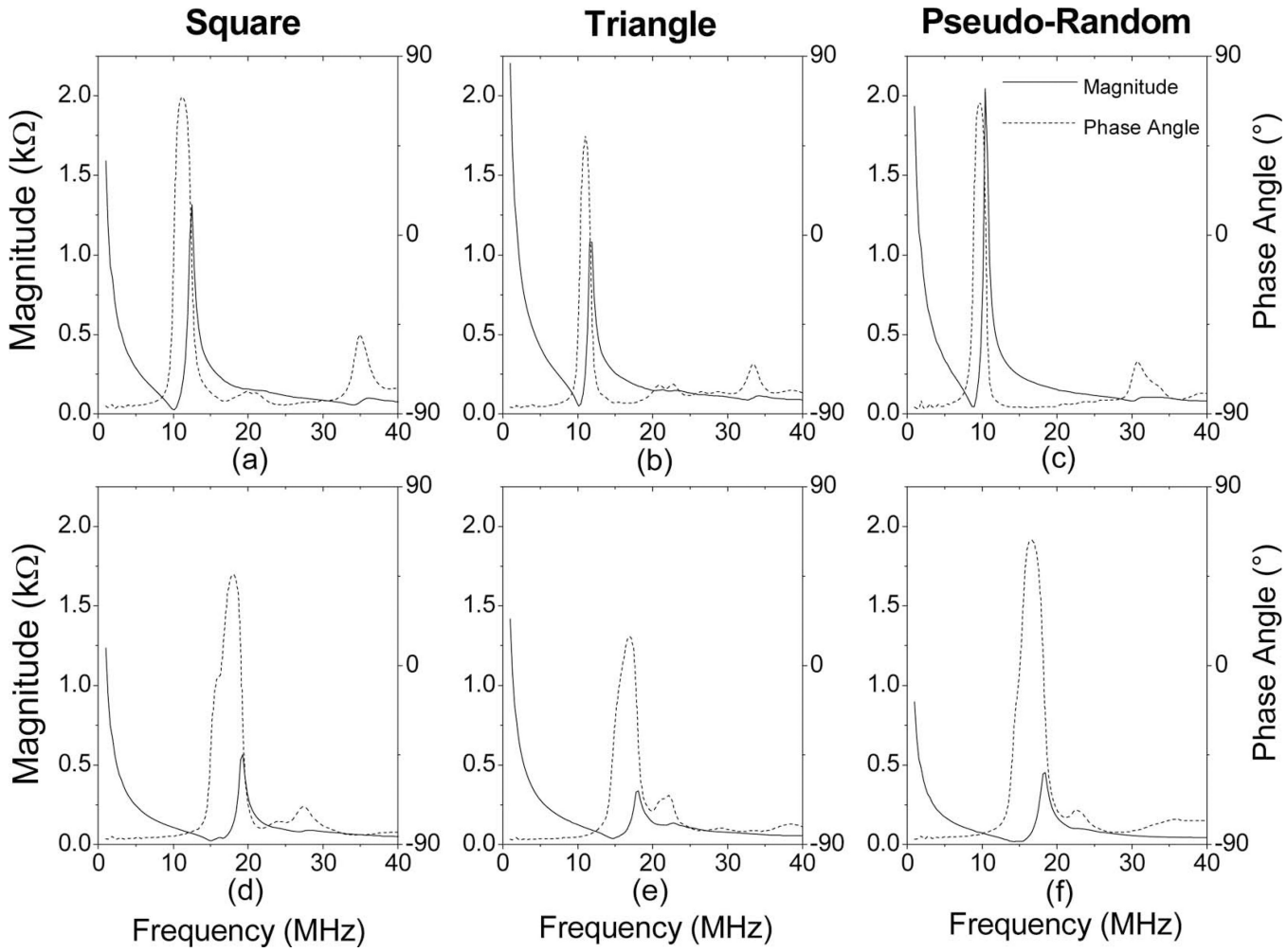

Fig. 2.

Measured (solid line) electrical impedance and (dashed line) phase angle for the piezocomposites with different pillar geometries: at 10 MHz, (a) square, (b) triangle, and (c) pseudo-random, and at 15 MHz, (d) square, (e) triangle, and (f) pseudo-random.

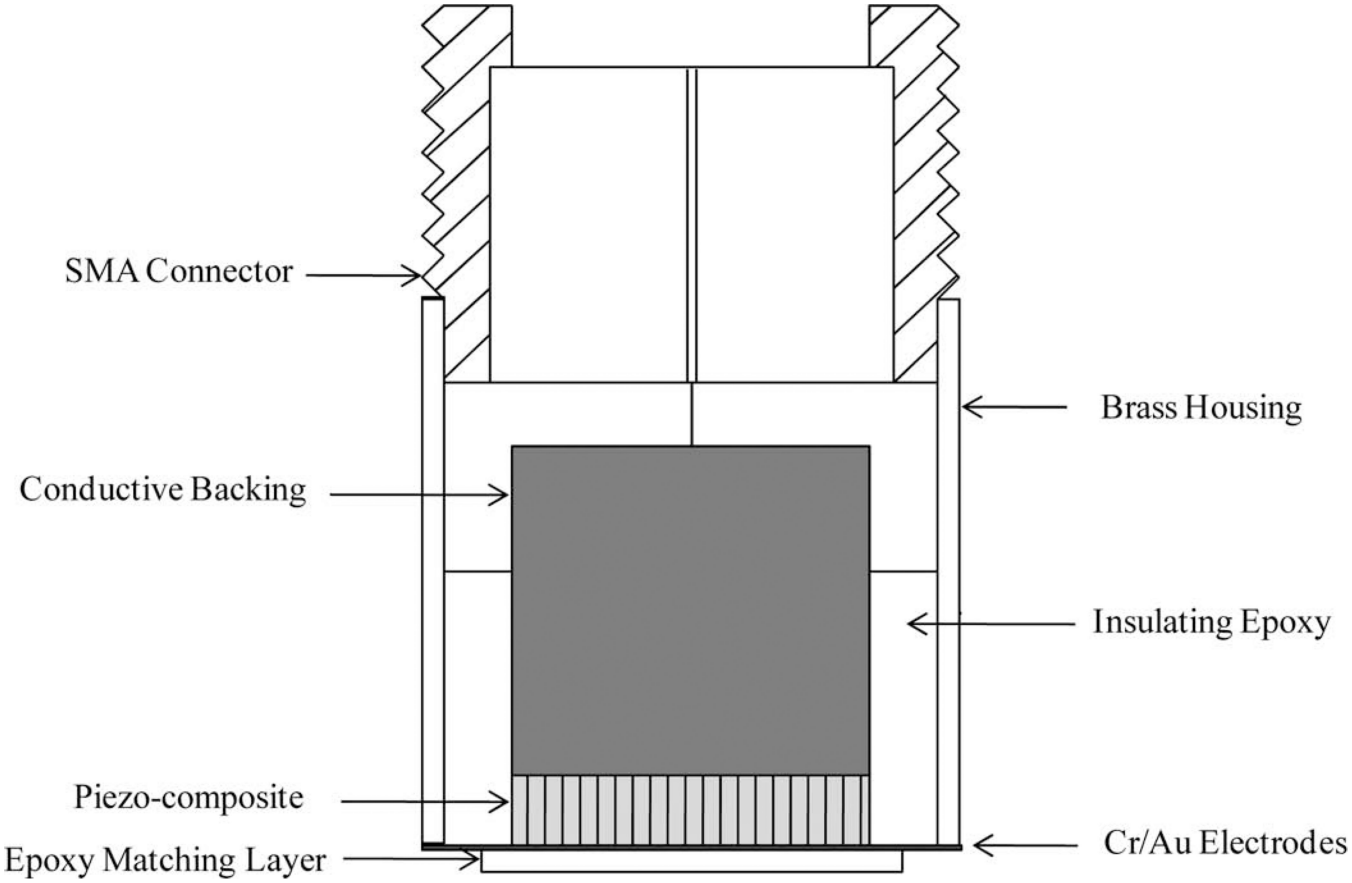

Fig. 3.
A cross-sectional drawing of the single-element ultrasound transducers.

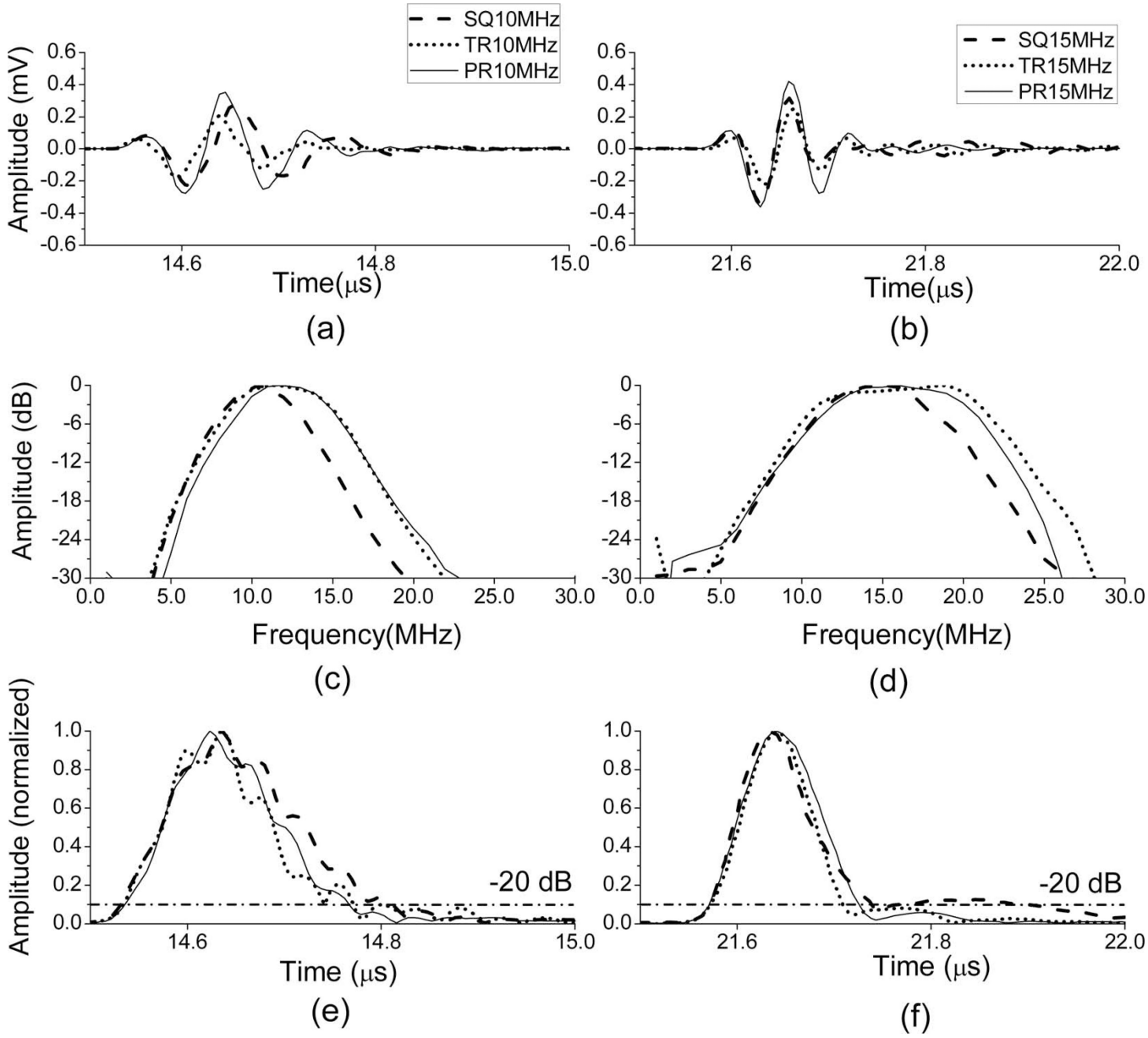

Fig. 4.

(a) Measured pulse–echo waveforms, (c) their spectra, and (e) envelopes at 10 MHz for the composite single-element ultrasound transducers. (b) Measured pulse–echo waveforms, (d) their spectra, and (f) envelopes at 15 MHz for the composite single-element ultrasound transducers.

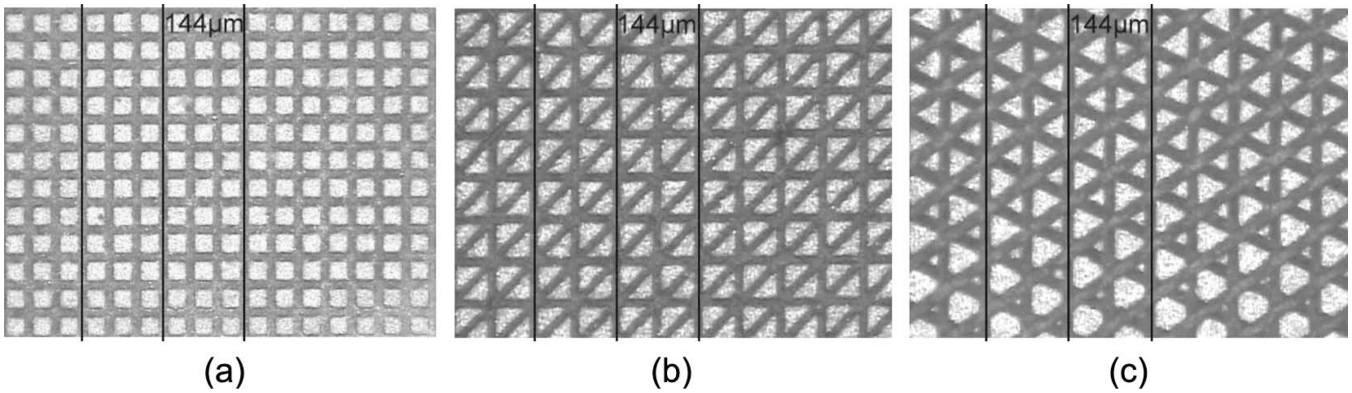

Fig. 5.
Sputtered 1–3 composites with different pillar geometries (removing the Cr/Au over the epoxy kerfs): (a) square, (b) 45° triangle, and (c) pseudo-random.

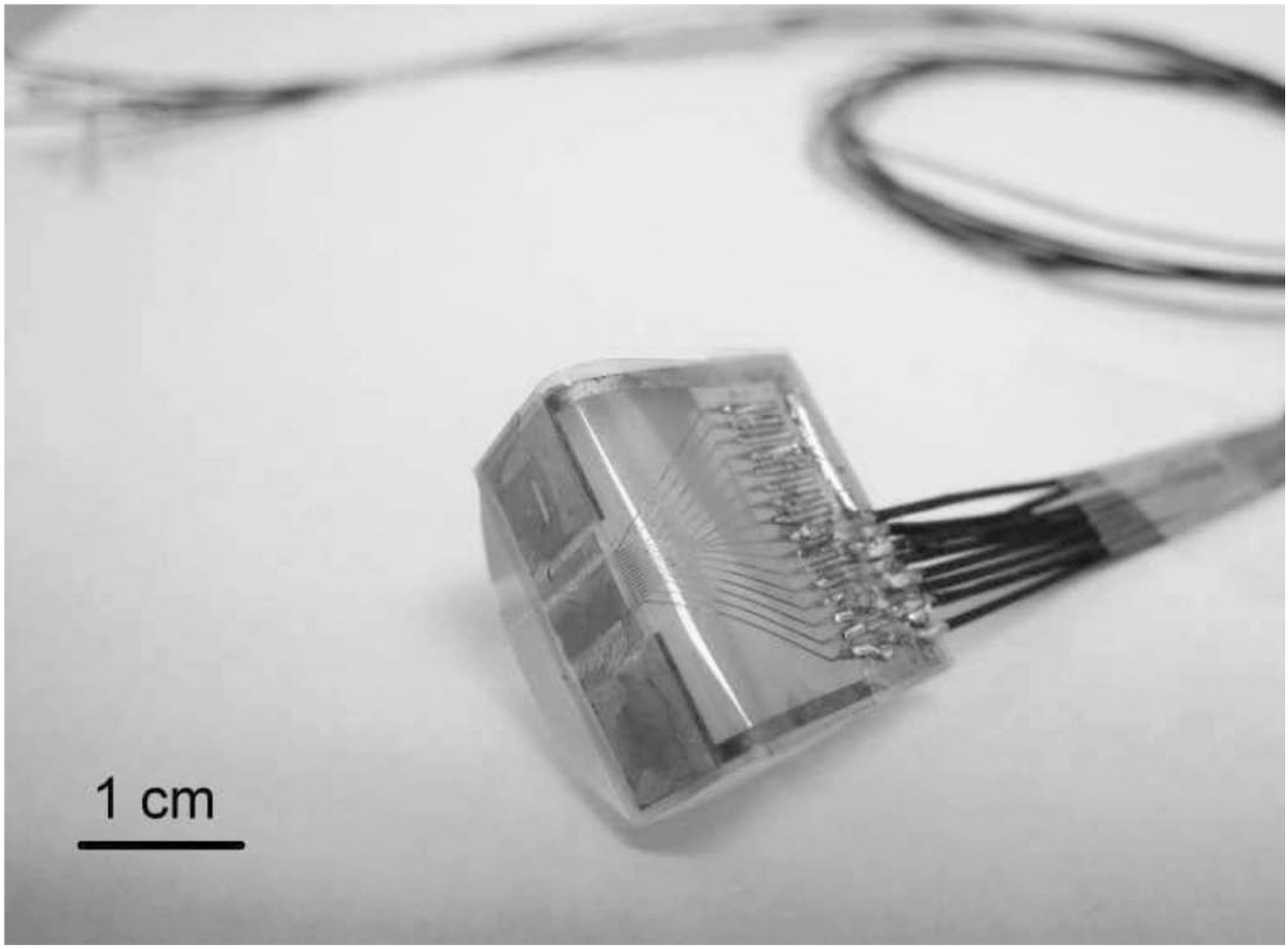

Fig. 6.
A photograph of the completed array subaperture.

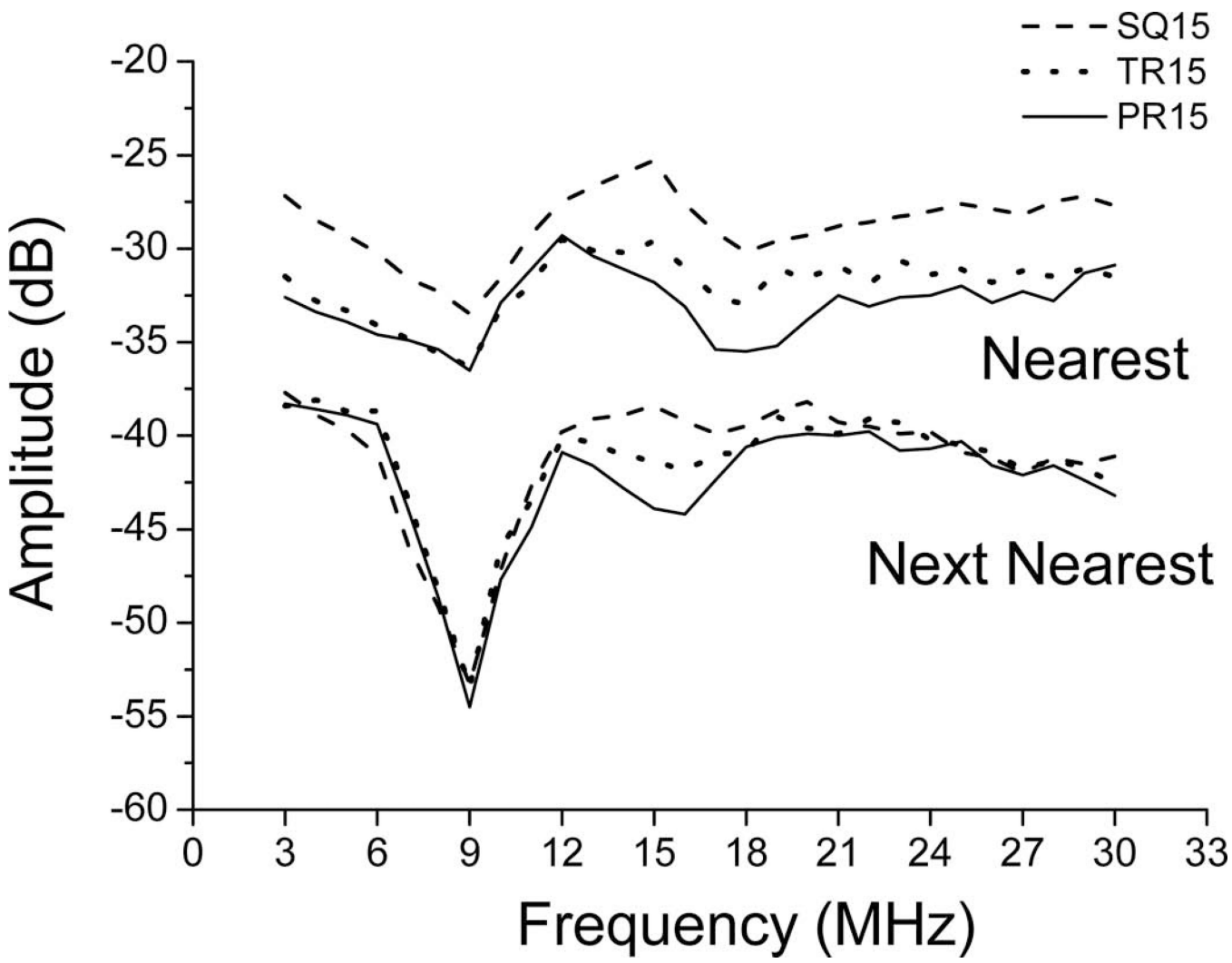

Fig. 7.

Average measured combined electrical and acoustical crosstalk between the nearest and next-nearest elements of the array subapertures with different pillar geometries.

TABLE I

Designed Parameters for the PZT-5H 1–3 Composites With Different Pillar Geometries for This Study.

	Center frequency (MHz)	Thickness (*H*) (μm)	Max. aspect ratio (*W*/*H*)	Pillar width (*W*) (μm)	Kerf (*K*) (μm)	Pitch (*P*) (μm)	Ceramic volume fraction (%)
Square	10	165	0.29	34	14	48	50
45° Triangle	10	165	0.33	38	14	52	46
Pseudo-random	10	165	0.35	57	14	71	49
Square	15	110	0.44	34	14	48	50
45° Triangle	15	110	0.49	38	14	52	46
Pseudo-random	15	110	0.52	57	14	71	49

IEEE Trans Ultrason Ferroelectr Freq Control. Author manuscript; available in PMC 2013 August 23.

TABLE II

Average Measured Material Properties for the PZT-5H 1–3 Composites With Different Pillar Geometries Manufactured for This Study.

	Thickness μm	k_t	tan δ	Q_m	α (dB/mm)	$\varepsilon_{33}^S/\varepsilon_o$	V_1 (m/s)
SQ 10-MHz	164 (0.5)	0.57 (0.012)	0.12 (0.009)	44.8 (3.8)	1.85 (0.15)	472 (25)	4037 (35)
TR 10-MHz	165 (0.7)	0.52 (0.018)	0.20 (0.013)	41.9 (3.1)	1.97 (0.28)	484 (33)	3653 (42)
PR 10-MHz	161 (0.3)	0.62 (0.020)	0.15 (0.008)	33.1 (4.3)	2.84 (0.22)	493 (15)	3850 (39)
SQ 15-MHz	111 (0.7)	0.58 (0.011)	0.11 (0.010)	21.6 (2.9)	5.68 (0.19)	501 (37)	4173 (55)
TR 15-MHz	113 (0.8)	0.51 (0.023)	0.20 (0.007)	22.7 (3.7)	5.31 (0.25)	457 (29)	3526 (47)
PR 15-MHz	110 (0.5)	0.61 (0.019)	0.16 (0.015)	25.1 (3.5)	4.93 (0.28)	520 (45)	4015 (59)

SQ = square; TR = 45° triangle; PR = pseudo-random. Values in parentheses are the standard deviations for the measured properties.

TABLE III

Measured Frequency Response Properties for the PZT-5H 1–3 Composites Transducers With Different Pillar Geometries.

	Center frequency (CF) (MHz)	Without a matching layer, −6-dB Bandwith (% CF)	With a matching layer, −6-dB bandwith (% CF)	V_{pp} (V)	−20-dB pulse length (ns)
SQ 10-MHz	10.5	48	54	0.48	282
TR 10-MHz	11.6	67	65	0.41	239
PR 10-MHz	11.8	60	61	0.60	230
SQ 15-MHz	15.8	55	58	0.62	172
TR 15-MHz	16.0	65	69	0.48	140
PR 15-MHz	15.9	63	66	0.75	148

SQ = square; TR = 45° triangle; PR = pseudo-random.

TABLE IV

Measured Insertion Loss (IL) and −20 dB Pulse Length (PL) for the 15-MHz Array Subapertures With Different Pillar Geometries.

		1	2	3	4	5	6	7	8	Mean
SQ	IL (db at 15 MHz)	−25.2	−26.1	−26.6	−24.8	−25.5	−24.8	−27.0	−25.5	−25.6 (0.81)
	−20-db Pl (ns)	195	206	205	193	210	202	198	213	202.7 (7.08)
TR	IL (db at 15 MHz)	−28.3	−27.5	−26.9	−27.2	−26.6	−27.7	−29	−28.1	−27.6 (0.78)
	−20-db Pl (ns)	156	145	140	153	153	142	163	158	151.2 (8.13)
PR	IL (db at 15 MHz)	−24.5	−25.3	−24.2	−24.8	−25.3	−22.3	−24.5	−22.8	−24.2 (1.10)
	−20-db Pl (ns)	142	150	148	155	144	135	128	149	143.8 (8.77)

SQ = square; TR = 45° triangle; PR = pseudo-random. Values in parentheses are the standard deviations for the measured properties.

Elements 1 to 8 of each array subaperture were measured to represent all of the elements.

IEEE Trans Ultrason Ferroelectr Freq Control. Author manuscript; available in PMC 2013 August 23.

TABLE V

Average Measured Combined Crosstalk (Electrical And Acoustical) for the 15-MHz Array Subapertures With Different Pillar Geometries.

	Adjacent elements at 15 MHz (dB)	Standard deviation (dB)	Next-nearest elements at 15 MHz (dB)	Standard deviation (dB)
SQ	−25.3	0.48	−38.4	0.36
TR	−29.6	0.61	−41.3	0.32
PR	−31.8	0.65	−43.9	0.43

SQ = square; TR = 45° triangle; PR = pseudo-random.

Elements 1 to 8 of each array subaperture were measured to represent all of the elements.